How Pulsars Shine

calculating
understanding
} pulsars

Results :

→ can calculate weak* (to be defined) pulsars, standard candles

→ should be able to calculate non-weak pulsars

→ rough understanding of weak pulsars

No Results :

→ radio, other non-γ

→ ions

→ ~~[illegible]~~ understanding of strong pulsars

Weak and non-weak pulsars

I, I' – force-free zone

I' – corotation zone

II – radiation zone

Here colliding Poynting fluxes annihilate into curvature radiation

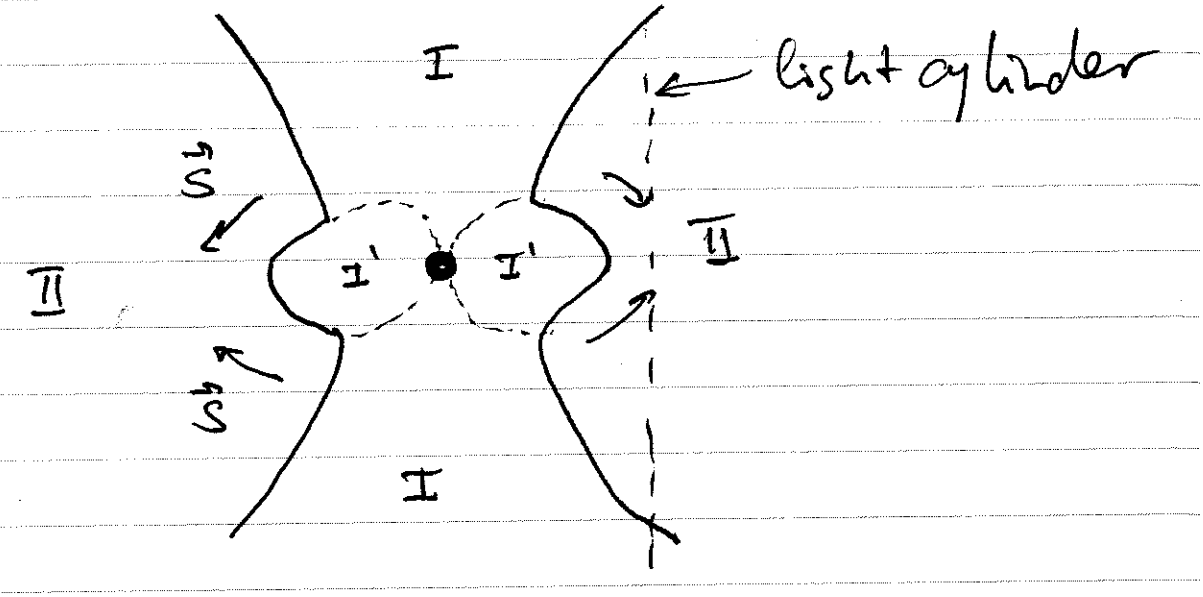

weak : negligible

non-weak : non-negligible

particle production in II

(compared to $\Omega \hbar_{GJ}$)

what is needed to calculate the pulsar?

$$\vec{E}, \quad \vec{B}, \quad \rho_{\pm}$$

$$\begin{cases} \dot{\vec{B}} = -\nabla \times \vec{E} \\ \dot{\vec{E}} = \nabla \times \vec{B} - \vec{j} \end{cases}$$

$$\vec{j} = \begin{cases} \rho_+ \vec{v}_+ - \rho_- \vec{v}_- & , \text{ magn} \\ \sigma(\vec{E} + \vec{v} \times \vec{B}) & , \text{ star} \end{cases}$$

$$\dot{\rho}_{\pm} + \nabla \cdot (\rho_{\pm} \vec{v}_{\pm}) = 0$$

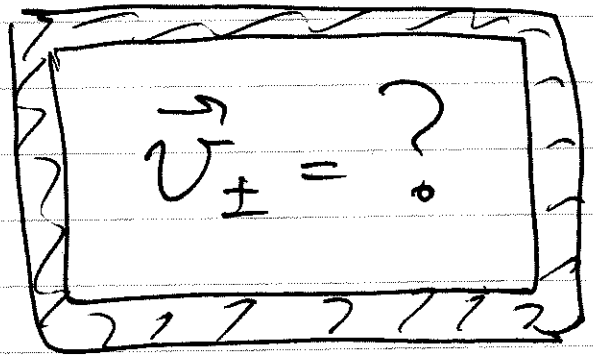

$\Downarrow$

(radiation too)

Aristotelian Electrodynamics = Electrodynamics of Massless Charges

Newt: $\vec{a} = \vec{a}(\vec{F})$

Arist: $\vec{v} = \vec{v}(\vec{F})$

Lorentz force = Radiation damping

$$\vec{v}_\perp = \frac{\vec{E}\times\vec{B} \pm (B_0\vec{B} + E_0\vec{E})}{B^2 + E_0^2}$$

proper fields E_0, B_0

scalar pseudoscalar

$$B_0^2 - E_0^2 = \vec{B}^2 - \vec{E}^2$$

$$B_0 E_0 = \vec{B}\cdot\vec{E} \neq 0$$

$$E_0 \geq 0$$

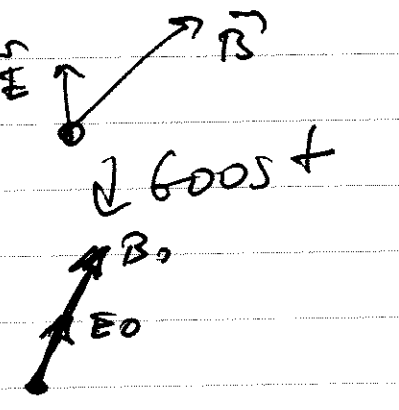

B. Finkbeiner, H. Herold, T. Ertl, H. Ruder

Radiation

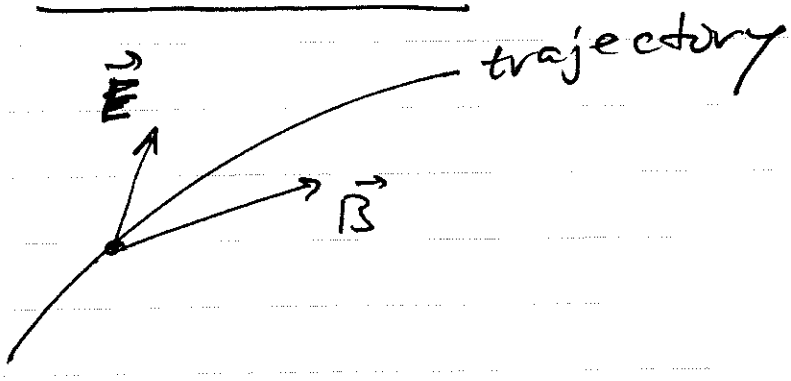

curvature of traj.

$$\pm e c \vec{v}_{\pm} \cdot \vec{E} = e c E_0 = \frac{2}{3} e^2 c K^2 \gamma^4$$

$\gamma = \ldots$

$\Downarrow$

synch. , critical energy

$$\mathcal{E}_c = \frac{3}{2} c \hbar K \gamma^3$$

Production of Charges

Ruderman, Sutherland Stroke

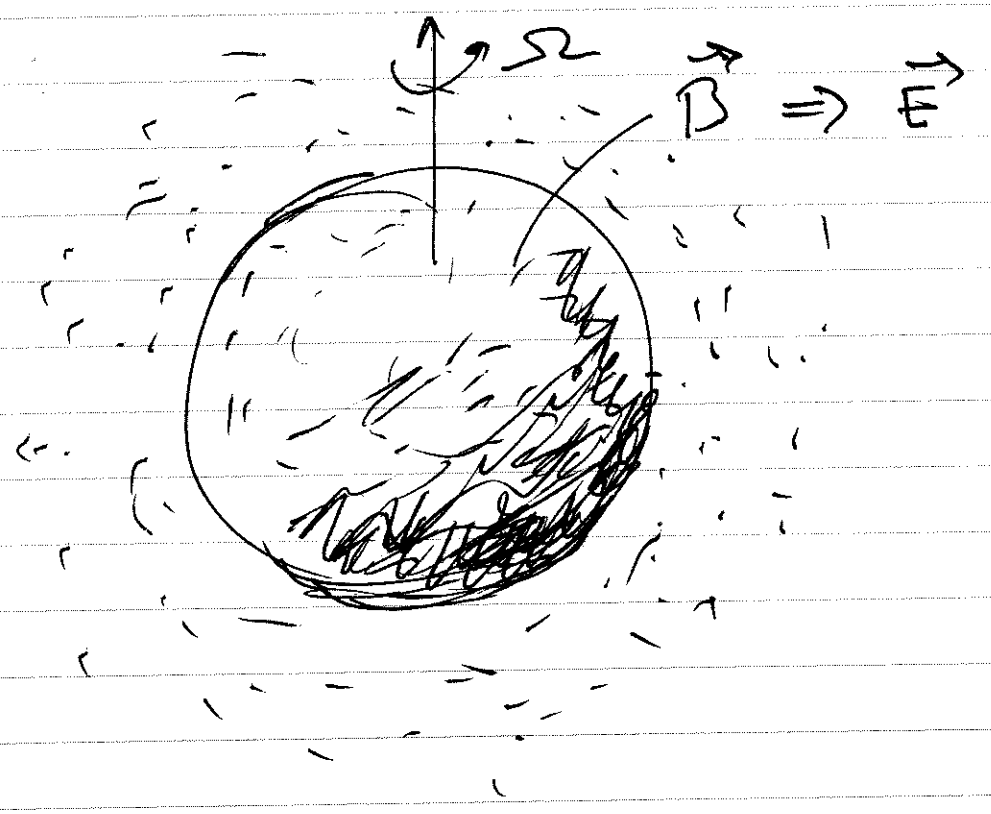

$E < E_{schwinge}$, but

still unstable:

$$\begin{cases} \gamma|_{B_0} \rightarrow e^+ + e^- \\ e^\pm|_{E_0, B_0} \rightarrow e^\pm + \gamma \end{cases}$$

only works close to the star, even for Crab (in I)

Charge Production in Non-Weak

in Π :

same as before but $B_0 \to X$

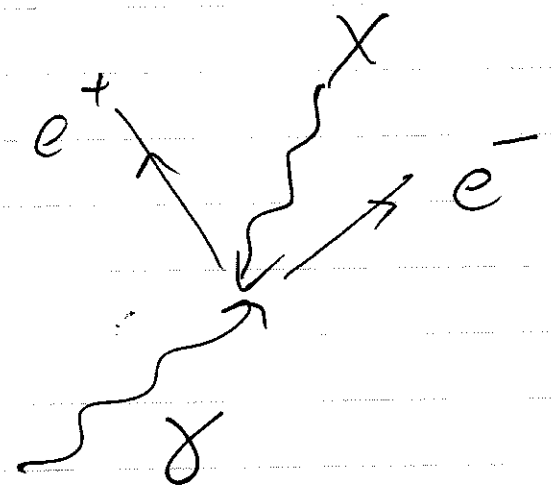

X - from J/ψ

X - from $e^{\pm}$ (synchr.)

(about 1/2 of Fermi Rulers)

Understanding: why FFE is not enough?

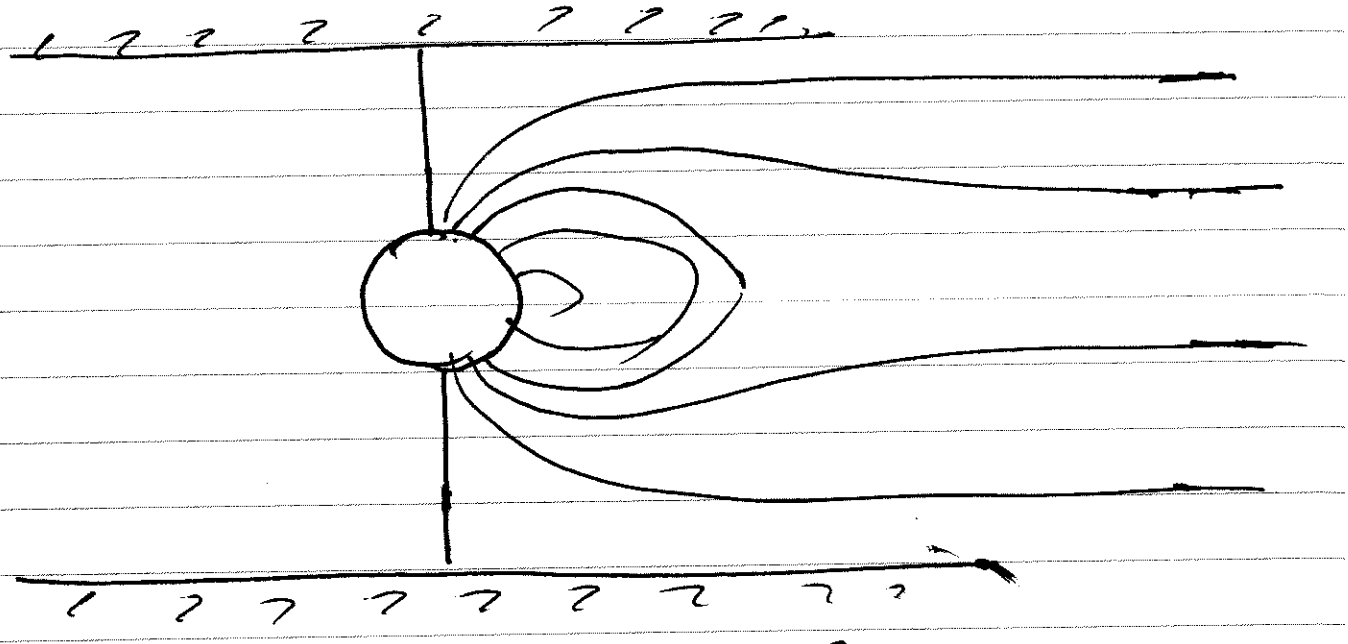

here $E_z = \text{const}$

$B_r, B_\theta \propto \frac{1}{r}$

$\left(S \propto \frac{1}{r} \right)$

$\Rightarrow$ inevitable become non. FFE

Understanding: Why FFE is OK in I?

FFE from AE

$$\vec{J}_{FFE} = \frac{(\nabla\cdot\vec{E})\,\vec{E}\times\vec{B} + \vec{B}\cdot(\nabla\times\vec{B}\cdot\vec{B} - \nabla\times\vec{E}\cdot\vec{E})}{B^2}$$

$$\vec{J}_{AE} = \frac{(\nabla\cdot\vec{E})\,\vec{E}\times\vec{B} + \rho(B_0\vec{B} + \varepsilon_0\vec{E})}{B^2 + \varepsilon_0^2}$$

$$\rho = \rho_+ + \rho_-$$

$$(\nabla\cdot\vec{E} = \rho_+ - \rho_-)$$

AE:

$\vec{E}, \vec{B}$: 6

FFE:

$\vec{E}, \vec{B}, \vec{E} \perp \vec{B}$: 5

but now

$$B_0 = s|B_0|$$

$$|B_0|^2 = B^2 - E^2$$

but $\langle s \rangle$ is $+1$

arbitrary $[-1, 1]$

6

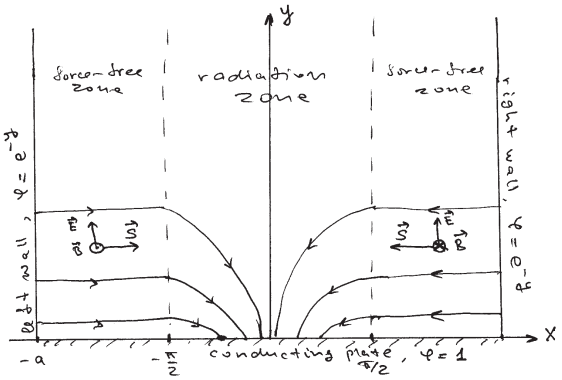

FIG. 2: The Device.

some electrons can still be pulled out at a rate needed to sustain the saturation.

We start off without any charges inside the Device, with $B = 0$, and with potential electric field $\mathbf{E} = -\nabla\phi$ which is given by $\nabla^2\phi = 0$ and the boundary values of ϕ. The walls start to emit electrons creating B and changing $\mathbf{E}$, as described by Maxwell equations (9) (with appropriate boundary conditions at the walls describing the electron pull-out rate).

D. Exact Solution

Assume that the Device does saturate. The resulting fields should satisfy stationary AE equations of §IV B. One can check that the following expressions do solve the equations and satisfy the boundary conditions specified above:

$$\phi(x,y) = e^{-y}, \tag{18}$$

$$B(x,y) = \begin{cases} -e^{-y} sign(x), & |x| > \frac{\pi}{2}; \\ -e^{-y}\sin(x), & |x| < \frac{\pi}{2}. \end{cases} \tag{19}$$

The domain $\frac{\pi}{2} < |x| < a$ is a force-free zone. Here the Grad-Shafranov equations (14, 15) are obeyed:

$$E_0 = 0, \quad B = \pm\phi, \quad \nabla^2\phi = \phi = B\frac{dB}{d\phi}. \tag{20}$$

The domain $|x| < \frac{\pi}{2}$ is a radiation zone. Here the non-force-free stationary AE equations (16, 17) are obeyed

$$E_0 = e^{-y}\cos(x), \tag{21}$$

$$\nabla\phi\cdot\nabla B = \partial_y\phi\partial_y B = \phi B = B\nabla^2\phi, \tag{22}$$

$$\hat{z}\cdot\nabla\phi\times\nabla B = -\partial_y\phi\partial_x B = -E_0\nabla^2\phi. \tag{23}$$

E. Discussion

The electromagnetic field and the corresponding Poynting fluxes in the force-free zones are shown in Fig.(2). In the left force-free zone electrons are moving to the right (along the lines of constant B shown in the figure). In the right force-free zone electrons are moving to the left.

The two electron beams carrying the Poynting fluxes are so polarized (opposite signs of B with collinear $\mathbf{E}$), that if they were to interpenetrate, a purely-electric region would have been created, where the electrons would have to move strictly down, rather than towards each other. A radiation zone must therefore separate the two force-free zones.

In the radiation zone, the Poynting flux remains parallel to the x-axis, flowing towards the y-axis, but none of it reaches the y-axis: $\mathbf{S} = (E_y B, -E_x B, 0) = (-e^{-2y}\sin(x), 0, 0)$. The entire Poynting flux gets annihilated into curvature radiation.

To discuss radiation, it makes sense to restore dimensions. We can do it by prescribing the wall potential as $\phi = FRe^{-y/R}$ where F has dimensions of electromagnetic field and R has dimensions of length. Then the curvature of electron trajectories in the radiation zone is $\sim R^{-1}$, the proper electric field is $\sim F$. According to the formulas of §III, the Device emits curvature photons of characteristic energy

$$E_{\rm c} \sim c\hbar e^{-3/4}F^{3/4}R^{1/2}. \tag{24}$$

Calling $L \sim cF^2R^2$ the power, erg/s, we get (as we should) the formula [1] expressing the photon cutoff energy $E_{\rm c}$ in terms of the power L and the size of the emitting region R:

$$E_{\rm c} \sim \frac{mc^2}{\alpha}{\rm Ar}^{3/8}, \tag{25}$$

where m is the mass of electron, α is the fine structure constant,

$${\rm Ar} \equiv \frac{L}{L_e}\left(\frac{R}{r_e}\right)^{-2/3}, \tag{26}$$

is the Aristotle number of the Device, $r_e = \frac{e^2}{mc^2} = 2.8\times 10^{-13}$cm is the classical electron radius and $L_e = \frac{mc^3}{r_e} = 8.7\times 10^{16}$erg/s is the "classical electron luminosity". AE is applicable at large Aristotle numbers,

$${\rm Ar} \gg 1. \tag{27}$$

V. CONCLUSION

- Pulsars shine by annihilating colliding Poynting Fluxes into curvature radiation.
- To solve a pulsar one can use AE.

II. MAGNETOSPHERE

First solve Maxwell equations

$$\dot{\mathbf{B}} = -\nabla \times \mathbf{E}, \tag{3}$$

$$\dot{\mathbf{E}} = \nabla \times \mathbf{B} - \mathbf{j}, \tag{4}$$

in entire space. The current $\mathbf{j}$ is given by two different expressions, which we call Ohm's laws, inside and outside the star of radius R_s.

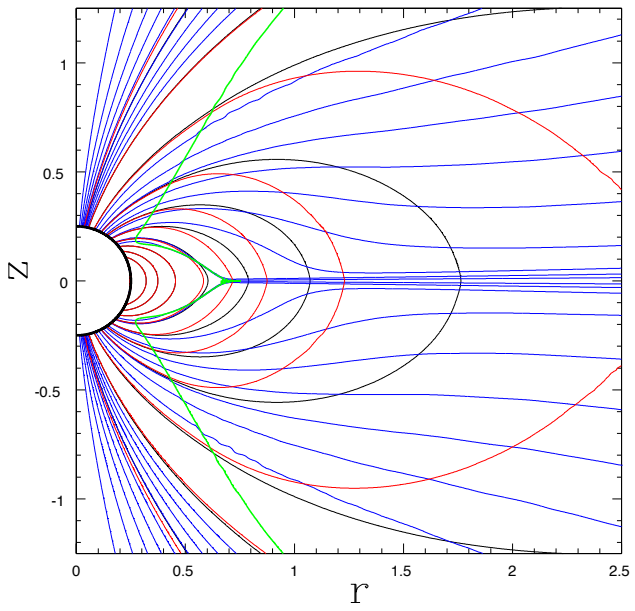

FIG. 1: Thin blue: A, integer multiples of $0.1A_{\max}$, $A_{\max} = 0.25$. Black and thin red: ψ and ϕ, 0.1,0.2, and integer multiples of 0.4. Thick green: the radiation zone boundary.

Inside the star, for spherical radii $R < R_s$, use the standard Ohm's law (in a rotating frame, angular velocity Ω) plus a fixed external toroidal current. The conductivity of the star is arbitrary, but $\gg 1/R_s$. The value and poloidal profile of the external current are arbitrary; they just determines the magnetic moment of the star μ; and μ scales out of the final results which will be given in terms of the pulsar observables: the spin-down power $L_{\rm sd}$ and the angular velocity of the star Ω.

Outside the star, $R > R_s$, use the following Ohm's law

$$\mathbf{j} = \frac{\rho\mathbf{E}\times\mathbf{B} + |\rho|(B_0\mathbf{B} + E_0\mathbf{E})}{B^2 + E_0^2}, \tag{5}$$

where

$$\rho \equiv \nabla \cdot \mathbf{E} \tag{6}$$

is the charge density.

Start with initial fields equal to zero. Regularize Maxwell equations (3) by small diffusivities $\eta\nabla^2\mathbf{B}$ and $\eta\nabla^2\mathbf{E}$ with $\eta \ll R_s$. Regularize the Ohm's law (5) by $E_0 \to E_0 + \epsilon$ with $\epsilon \ll$ the characteristic magnetic field value.

After a while the electromagnetic field saturates at what is shown in Fig.1. All results (unless specified otherwise) are given in "pulsar units":

$$c = \Omega = R_{\rm lc} = \mu = 1, \tag{7}$$

where $R_{\rm lc} = c/\Omega$ is the light cylinder radius.

In cylindrical coordinates, (r, θ, z), the saturated fields depend only on r and z and can be written as

$$\mathbf{E} = (-\partial_r\phi, 0, -\partial_z\phi)\,, \tag{8}$$

$$\mathbf{B} = \frac{1}{r}\,(-\partial_z\psi, A, \partial_r\psi)\,. \tag{9}$$

The electric field is represented by the electrostatic potential ϕ. The poloidal magnetic field is represented by the "magnetic stream function" ψ, equal to the θ-component of vector potential divided by r. The toroidal magnetic field is represented by the quantity A equal to twice the integrated poloidal current.

The thick green line in Fig.1 is the boundary between the force-free zone and the radiation zone. In the force-free zone, which lies inside the green line, $E_0 = 0$. In the radiation zone, which lies outside the green line, $E_0 > 0$.

The electric current flows along magnetic surfaces $A = const$. It is seen that the current flows everywhere in the radiation zone, while part of the force-free zone is free from poloidal current: this is the corotation zone, where the charges just rotate with the angular velocity of the star Ω.

Calculating the Poynting flux emanating from the star, $L_{\rm sd} = \frac{1}{2}\oint d\phi A$, we get the spin-down power

$$L_{\rm sd} \approx 0.3\frac{\mu^2\Omega^4}{c^3}, \tag{10}$$

which is well below the standard force-free pulsar luminosity[2].

We must state that our numerical simulation has insufficient resolution (we use the same primitive code as in [4] except that now we calculate the electric current from the Ohm's law instead of particle densities). It appears that one needs a star smaller than our $R_s = 0.25$ and a simulation box larger than our 5x10. As it is, our simulation results do not quite converge even at our ultimate 1600x3200 resolution. To take a crude guess, our numerical values are perhaps ∼10% uncertain.

III. EMISSION

Given the electromagnetic field, one calculates emission as follows. The force-free zone does not radiate. In

[2] For the force-free pulsar (first calculated by [5], improved by [6], done by [7]), $L_{\rm sd} \approx \frac{\mu^2\Omega^4}{c^3}(1+\sin^2\theta)$, where θ is the spin-dipole angle. But as discussed at the end of §3.4 of [4], the very existence of force-free pulsars is questionable.

the radiation zone, the radiated power per unit volume is

$$q = c|\rho|E_0. \tag{11}$$

This power is emitted along

$$\mathbf{v} = \begin{cases} \mathbf{v}_+, & \rho > 0; \\ \mathbf{v}_-, & \rho < 0; \end{cases} \tag{12}$$

where $\mathbf{v}_\pm$ are from eq.(1). The power is emitted with synchrotron spectrum of critical photon energy

$$E_{\rm c} = (3/2)^{7/4} c\hbar e^{-3/4} E_0^{3/4} K^{-1/2}, \tag{13}$$

where the curvature K is given by

$$K = |\mathbf{v} \cdot \nabla \mathbf{v}|. \tag{14}$$

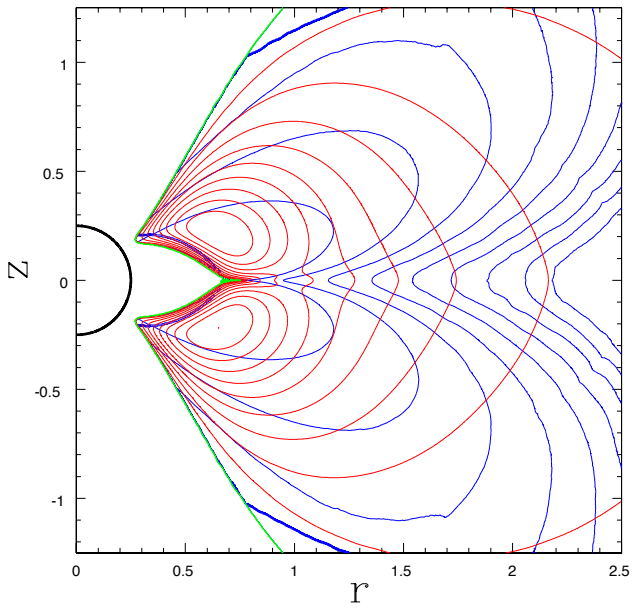

FIG. 2: Thin blue: radius of curvature to cylindrical radius ratio, $(Kr)^{-1}$, integer multiples of 0.5, increasing with increasing r. Red: E_0, integer multiples of $0.1E_{0\ \rm max}$, $E_{0\ \rm max} = 0.65$.

The proper electric field and the curvature are shown in Fig.(2). The radiated power density and the critical photon energy as a function of position are shown in Fig.(3). The insets show the power emitted at critical energies less than $E_{\rm c}$ as a function of $E_{\rm c}$ and the corresponding emission spectrum (obtained by convolving the spectrum of critical energies with the synchrotron spectrum); also shown is the PLEC fit (power law with exponential cutoff, $\frac{dN}{dE} \propto E^{-\Gamma} e^{-E/E_{\rm cut}}$).

The angle-integrated emission power corresponds to efficiency $\epsilon \approx 80\%$. The spectrum is close to PLEC with $\Gamma = 0.9$ (the PLEC fit to synchrotron emission gives $\Gamma{\rm synch} = 0.73$, but the distribution over critical energies $E_{\rm c}$ flattens it).

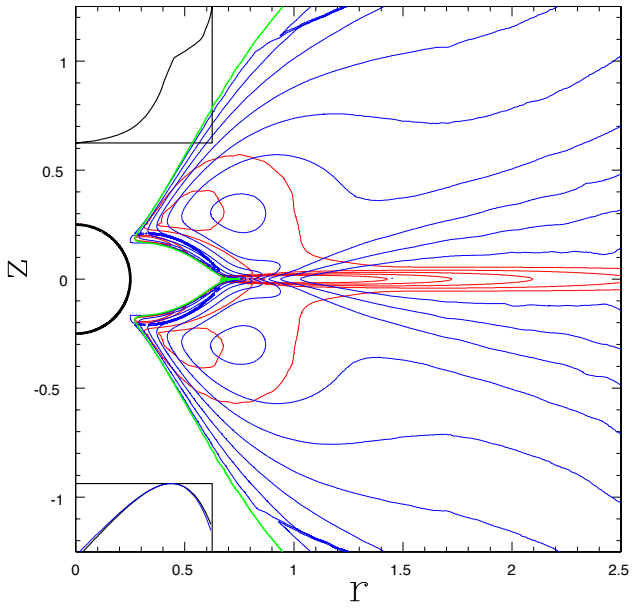

FIG. 3: Thin blue: critical energy of the photon spectrum $E_{\rm c}$, integer multiples of $0.1E_{\rm c\ max}$ with $E_{\rm c\ max} = 2.5\frac{mc^2}{\alpha}{\rm Ar}^{3/8}$. Red: r-normalized power density rq, in octaves, from 0.05 to 3.2. Upper inset: power distribution over critical energies – total power emitted at critical energies $< E_{\rm c}$ vs. $E_{\rm c}$. Lower inset: power spectrum, $\log(E^2\frac{dN}{dE})$ vs. $\log E$, and the PLEC fit (thin blue).

The cutoff photon energy for the angle-integrated emission is, in physical units,

$$E_{\rm cut} \approx 1.9\frac{mc^2}{\alpha}{\rm Ar}^{3/8}, \tag{15}$$

where $mc^2 = 0.511$MeV is the electron mass, $\alpha = \frac{e^2}{c\hbar} = \frac{1}{137}$ is the fine structure constant, and we have introduced the *Aristotle number* of a pulsar Ar,

$${\rm Ar} \equiv \frac{L_{\rm sd}}{L_e}\left(\frac{R_{\rm lc}}{r_e}\right)^{-2/3}, \tag{16}$$

where $r_e = \frac{e^2}{mc^2} = 2.8\times10^{-13}$cm is the classical electron radius and $L_e = \frac{mc^3}{r_e} = 8.7\times10^{16}$erg/s is the classical electron luminosity. As we show in §IV, AE is applicable to pulsars with ${\rm Ar} \gg 1$, which is true for all Fermi pulsars. In astrophysical notation, eq.(15) reads

$$E_{\rm cut} \approx 5.2 L_{34}^{3/8} P_{\rm ms}^{-1/4}{\rm GeV}, \tag{17}$$

which agrees with the crude estimate of [3].

Observed properties of emission are obtained by counting only photons emitted into a fixed infinitesimal solid angle. Let χ be the observation angle: the angle between the spin axis and the direction to the observer. Then we select only photons emitted by particles with

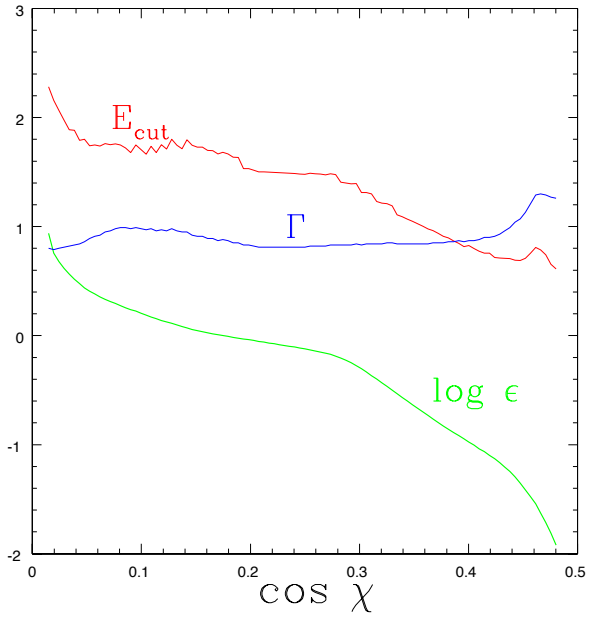

FIG. 4: Observed photon cutoff energy $E_{\rm cut}$, photon index Γ, and efficiency ϵ vs. the observation angle χ.

$|v_z| \approx \cos\chi$. We get the observed efficiency ϵ, photon index Γ, and photon cutoff energy $E_{\rm cut}$ shown in Fig.(4).

Serious comparison with observations is only possible after a 3D simulation. But Table I looks promising.

PSR	$P_{\rm ms}$	L_{34}	$E_{\rm cut}$	$E_{\rm cut}$, (17)	Γ	ϵ, %
0106	83	2.9	2.7 ± 0.6	2.6	1.2 ± 0.2	71^{+60}_{-31}
0357	444	0.6	0.8 ± 0.1	0.9	1.0 ± 0.1	...
0622	333	2.7	0.6 ± 0.1	1.8	0.6 ± 0.4	...
1057	197	3.0	1.4 ± 0.1	2.1	1.0 ± 0.1	14 ± 10
1741	414	0.9	0.9 ± 0.1	1.1	1.1 ± 0.1	22 ± 3
1836	173	1.1	2.0 ± 0.1	1.5	1.2 ± 0.1	180^{+200}_{-100}
1957	375	0.5	1.0 ± 0.2	0.9	1.3 ± 0.2	...
2030+4	227	2.2	1.7 ± 0.3	1.8	1.6 ± 0.1	...
2055	320	0.5	1.1 ± 0.1	0.9	1.0 ± 0.1	...
2139	283	0.3	1.3 ± 0.3	0.8	1.3 ± 0.2	...

TABLE I: All young Fermi pulsars with spin-down power $L_{34} < 3$, from [2], $E_{\rm cut}$ is in GeV. The fifth column calculates $E_{\rm cut}$ from eq.(17).

IV. AE AND WEAK PULSAR

Here we derive the equations used in §§II,III. We first derive AE and calculate radiation in AE. Then we show that the magnetosphere calculated in §II is realizable as an AE flow emanating from the star.

A. AE, radiation in AE

For a generic electromagnetic field, a one-parameter family of Lorentz frames exists at any event, such that **E** is parallel to **B** in these frames. Assume that in these frames a positive charge moves at the speed of light along **E** and a negative charge moves at the speed of light along $-\mathbf{E}$. Written in an arbitrary Lorentz frame, this gives the basic AE equation (1).

Of course, the charges actually move slower than light. The terminal Lorentz factor γ is reached when the curvature radiation power balances the accelerating power of E_0:

$$\pm ec\mathbf{v}_\pm \cdot \mathbf{E} = ecE_0 = \frac{2}{3}e^2cK^2\gamma^4, \qquad (18)$$

where the curvature of the trajectory K can be calculated using the approximate speed of light motion given by eq.(1). Knowing the terminal Lorentz factor γ, one gets the critical energy of the emitted photon spectrum (13).

The distance over which a charge needs to travel in order to get accelerated to the terminal Lorentz factor γ is $\sim \frac{\gamma mc^2}{eE_0}$. Demanding that this distance be much smaller than $R_{\rm lc}$, estimating the curvature as $K \sim R_{\rm lc}^{-1}$, and estimating the electric field from $L_{\rm sd} \sim cE_0^2R_{\rm lc}^2$, we get the AE applicability condition

$$\mathrm{Ar} \equiv \frac{L_{\rm sd}}{L_e}\left(\frac{R_{\rm lc}}{r_e}\right)^{-2/3} \gg 1. \qquad (19)$$

With the same estimates, the critical photon energy given by (13) is

$$E_{\rm c} \sim \frac{mc^2}{\alpha}\mathrm{Ar}^{3/8}, \qquad (20)$$

in agreement with the numerical result (15).

B. AE magnetosphere

In brief, the recipe of §§II,III works because plasma multiplicity in the radiation zone is zero, meaning that only a single charge species is present at any point. This allows to infer the particle density from the electric charge density and calculate the radiation. Zero multiplicity also means that the Ohm's law (5) is exact in the radiation zone. In the force-free zone eq.(5) is wrong, but the actual form of the Ohm's law in the force-free zone is irrelevant.

Consider what happens in real weak pulsars (as opposed to what happens in the calculation of §II). Near the star, the standard avalanche mechanism [8] keeps working to (nearly) nullify E_0. This requires permanent pair production in the near-star zone; and some of the charges then flow out, thus bringing the electric charge and electric current to the space around the star. Let $\rho_\pm$ be the e-normalized number densities of positrons and electrons,

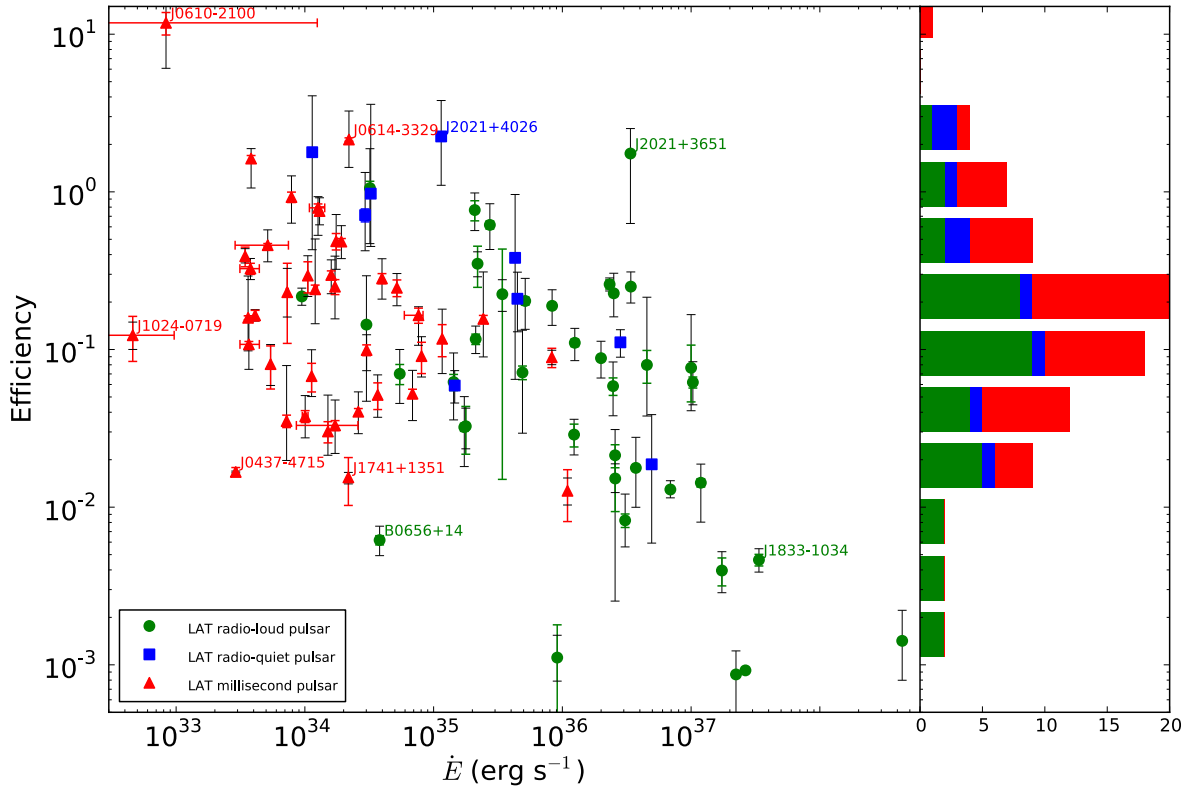

Fig. 10.— Gamma-ray efficiency $\eta = L_\gamma/\dot{E}$ versus spindown power $\dot{E}$. The error bars are as in Figure 9. The markers and the side histogram use the same color coding as in Figure 1.

large $\xi = 75\%$, produces a qualitative change: observed $\dot{E} = 12 \times 10^{33}$ erg s^{-1} decreases to corrected $\dot{E}^{\rm int} = 3 \times 10^{33}$ erg s^{-1}, right at the apparent deathline, and the efficiency changes from the lowest outlier amongst MSPs, to a low, but typical, $\eta = 1.7\%$.

The remaining four pulsars with $\xi > 60\%$ bear special discussion. Figure 11 plots lines of constant $\dot{E}$, L_γ, and transverse velocity v_T in μ vs. d space for different assumptions: $\dot{E} = 0$, $\dot{E} = L_\gamma$, and $\eta\dot{E} = L_\gamma$ with $\eta = 30$ %, at the high end of the observed range. The curve for $v_T = \mu d = 150$ km s^{-1} is the 3σ extremum of the MSP velocity distribution of Lyne et al. (1998). Faster recycled pulsars are possible, but unusual. Allowed (or favored) regions are to the left of the curves. The curve for $\dot{E} = 3 \times 10^{33}$ erg s^{-1} shows how an $\dot{E}$ value lower than those seen to date would compare with the other constraints. The shaded zones correspond to the measurements and their uncertainties adopted in this paper along

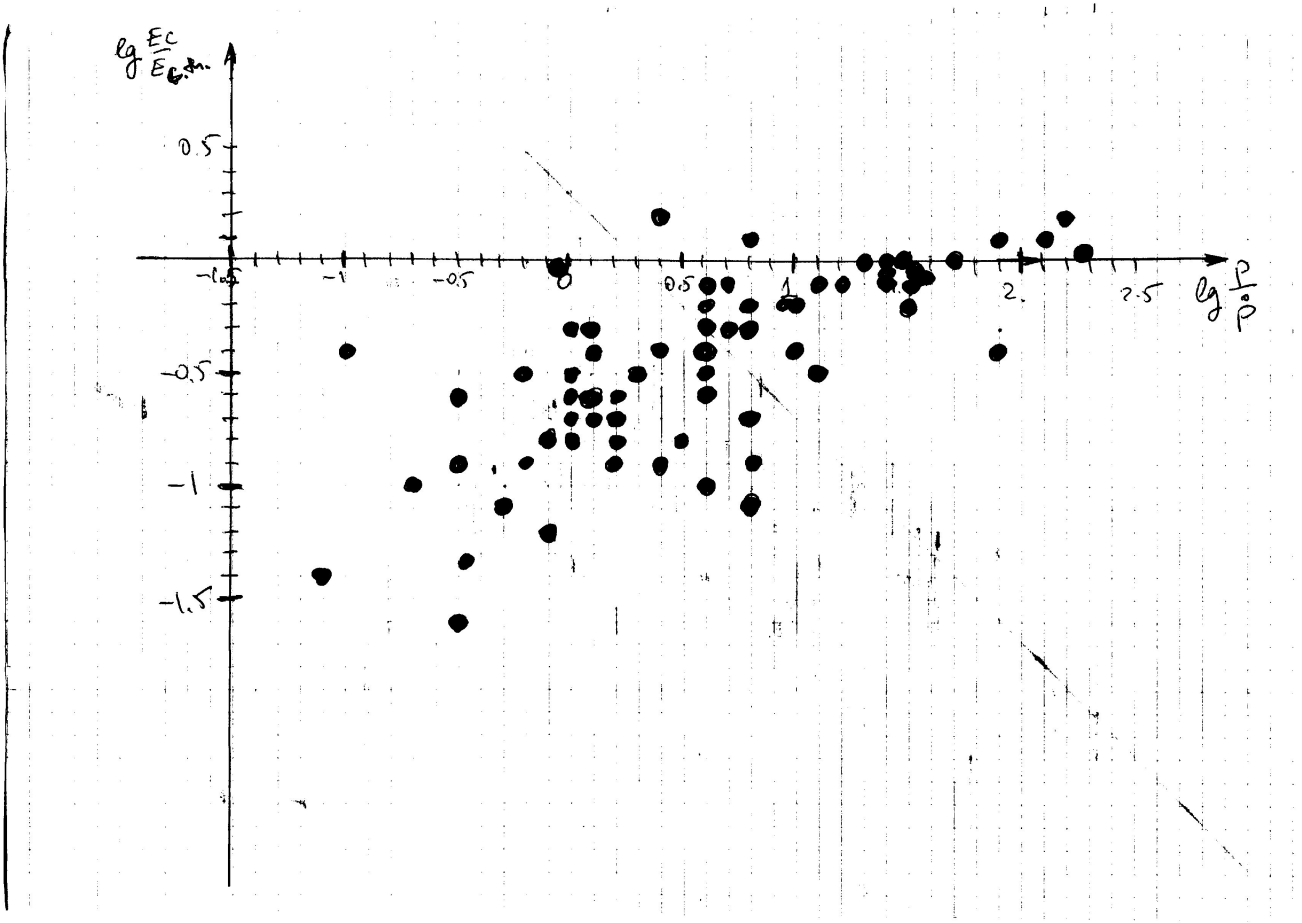
lg Ec / Ec th.
0.5
-1.5
-1
-0.5
0
0.5
1
2.
2.5
lg P / P0
-0.5
-1
-1.5

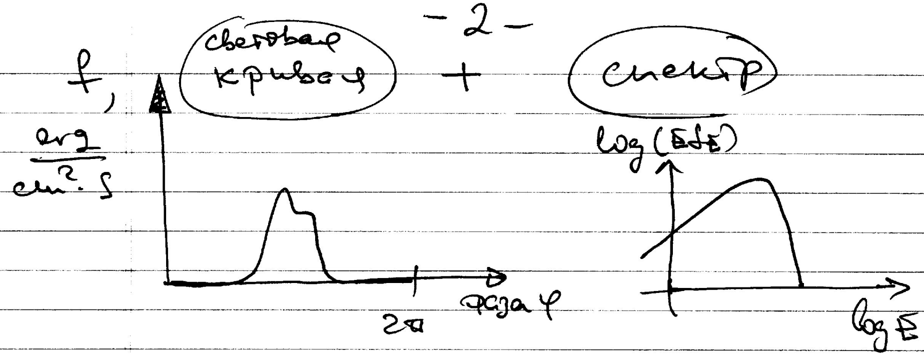

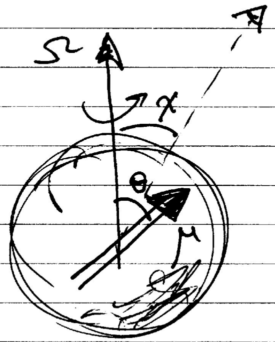

м. дип. момент μ

спин-диполь угол Θ

угол наблюдение χ

м. инерции I

расстояние d

(это и было сразу *в яв. виде)

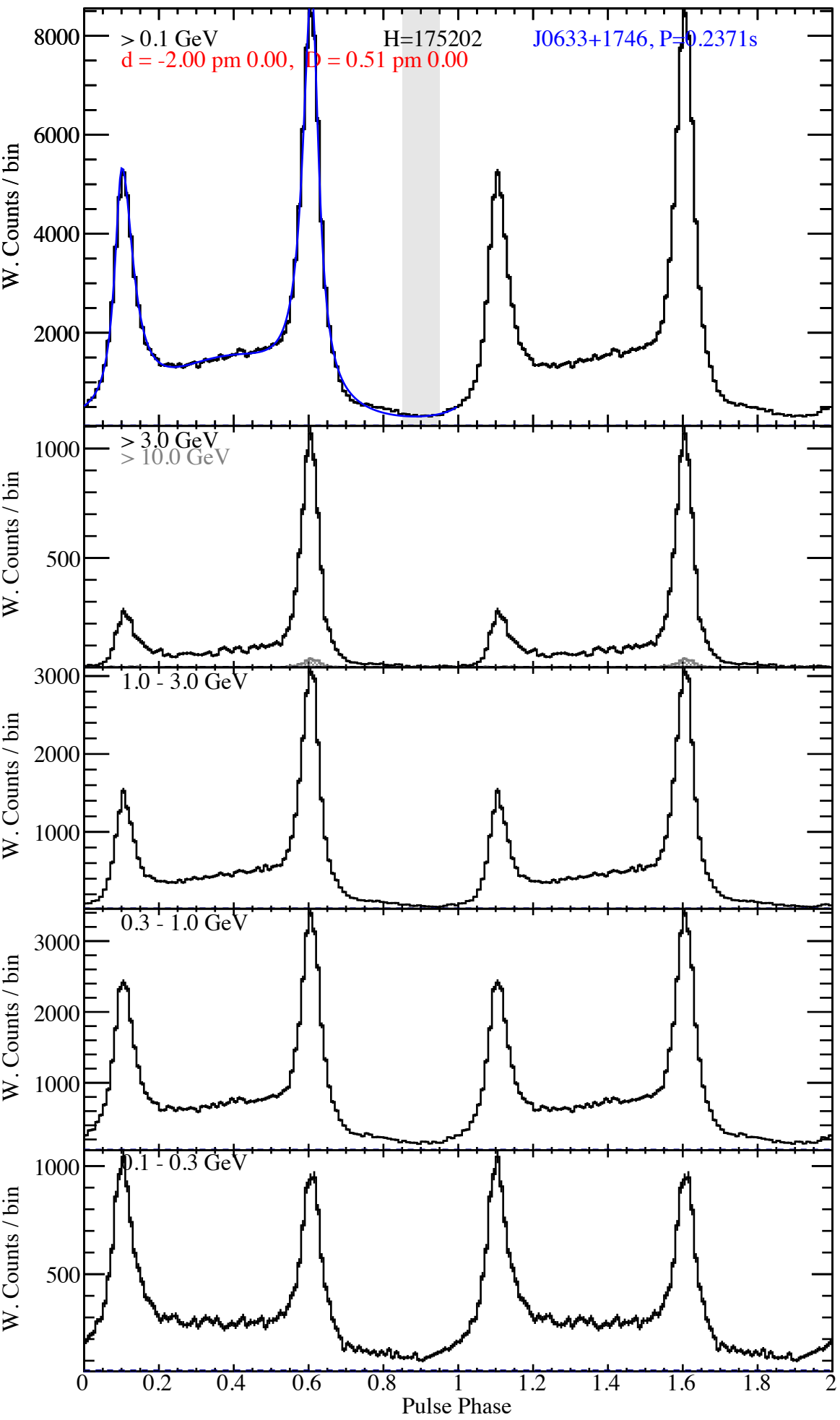
> 0.1 GeV
H=175202
J0633+1746, P=0.2371s
d = -2.00 pm 0.00, D = 0.51 pm 0.00
W. Counts / bin
> 3.0 GeV
> 10.0 GeV
1.0 - 3.0 GeV
0.3 - 1.0 GeV
0.1 - 0.3 GeV
Pulse Phase

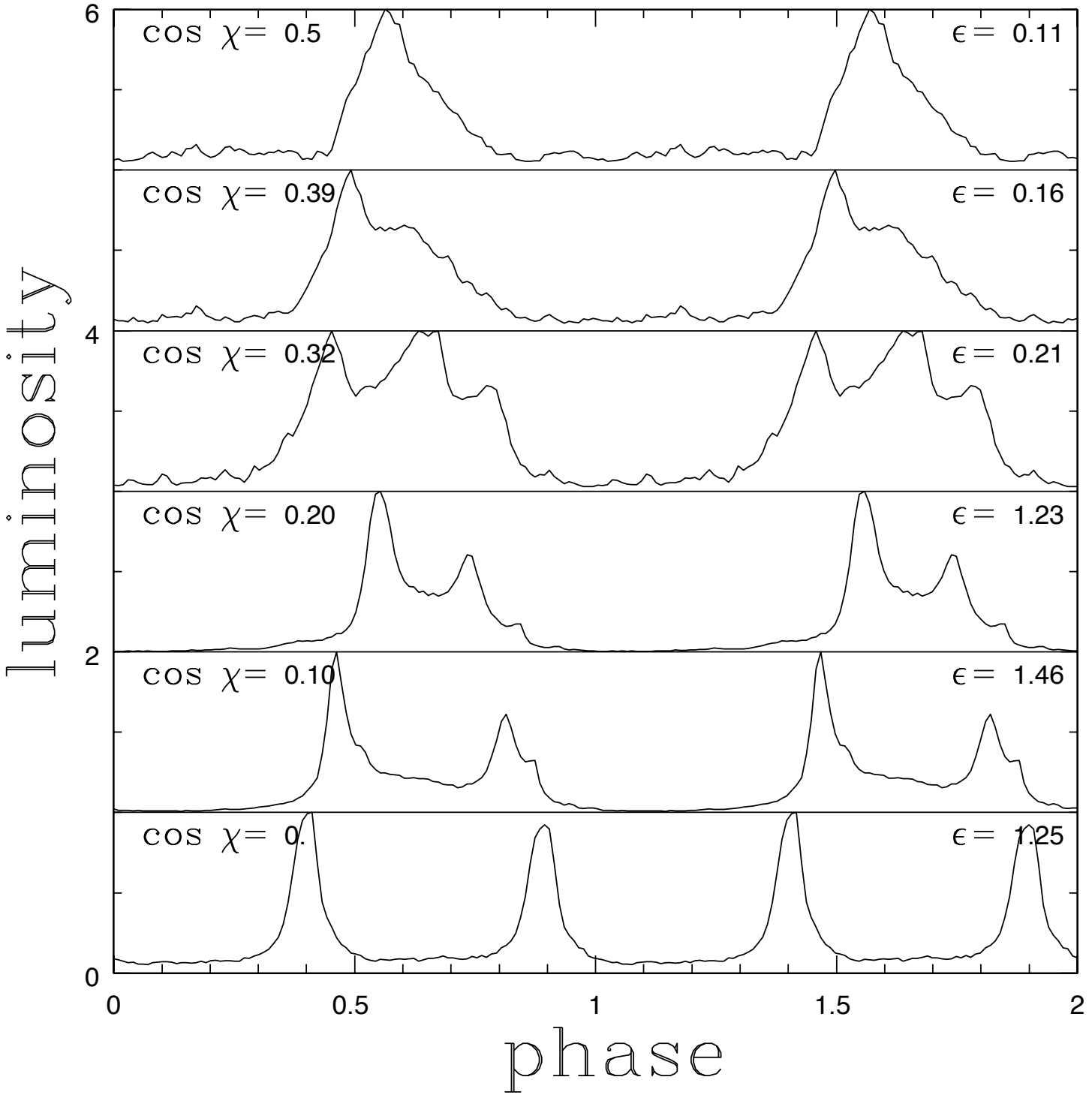
cos χ= 0.5
ϵ= 0.11
cos χ= 0.39
ϵ= 0.16
cos χ= 0.32
ϵ= 0.21
cos χ= 0.20
ϵ= 1.23
cos χ= 0.10
ϵ= 1.46
cos χ= 0.
ϵ= 1.25
luminosity
phase
0
2
4
6
0
0.5
1
1.5
2

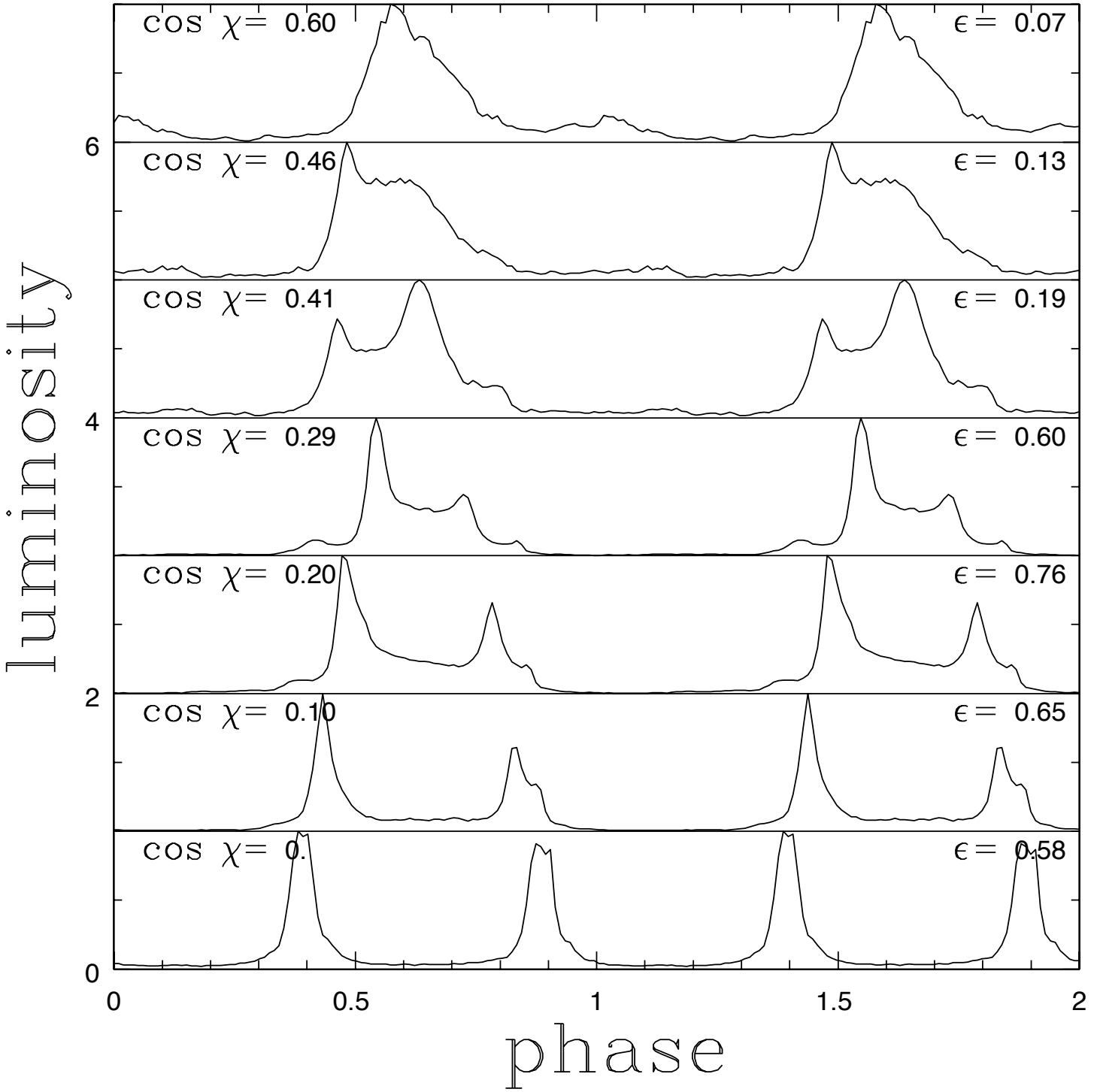
cos χ= 0.60
ϵ= 0.07
cos χ= 0.46
ϵ= 0.13
cos χ= 0.41
ϵ= 0.19
cos χ= 0.29
ϵ= 0.60
cos χ= 0.20
ϵ= 0.76
cos χ= 0.10
ϵ= 0.65
cos χ= 0.
ϵ= 0.58
luminosity
0
2
4
6
0
0.5
1
1.5
2
phase

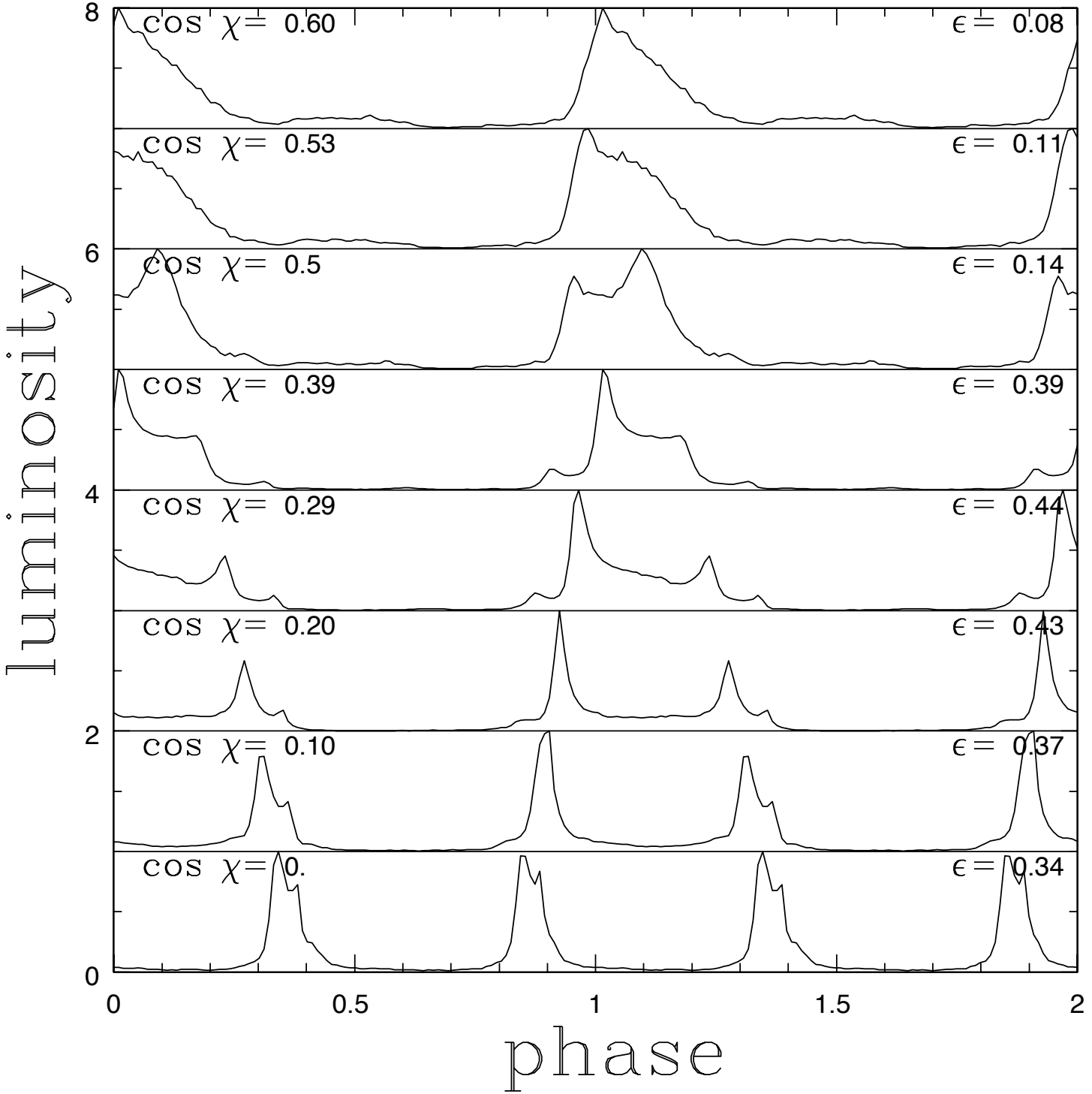
cos χ= 0.60
ϵ= 0.08
cos χ= 0.53
ϵ= 0.11
cos χ= 0.5
ϵ= 0.14
cos χ= 0.39
ϵ= 0.39
cos χ= 0.29
ϵ= 0.44
cos χ= 0.20
ϵ= 0.43
cos χ= 0.10
ϵ= 0.37
cos χ= 0.
ϵ= 0.34
luminosity
phase
0
2
4
6
8
0
0.5
1
1.5
2

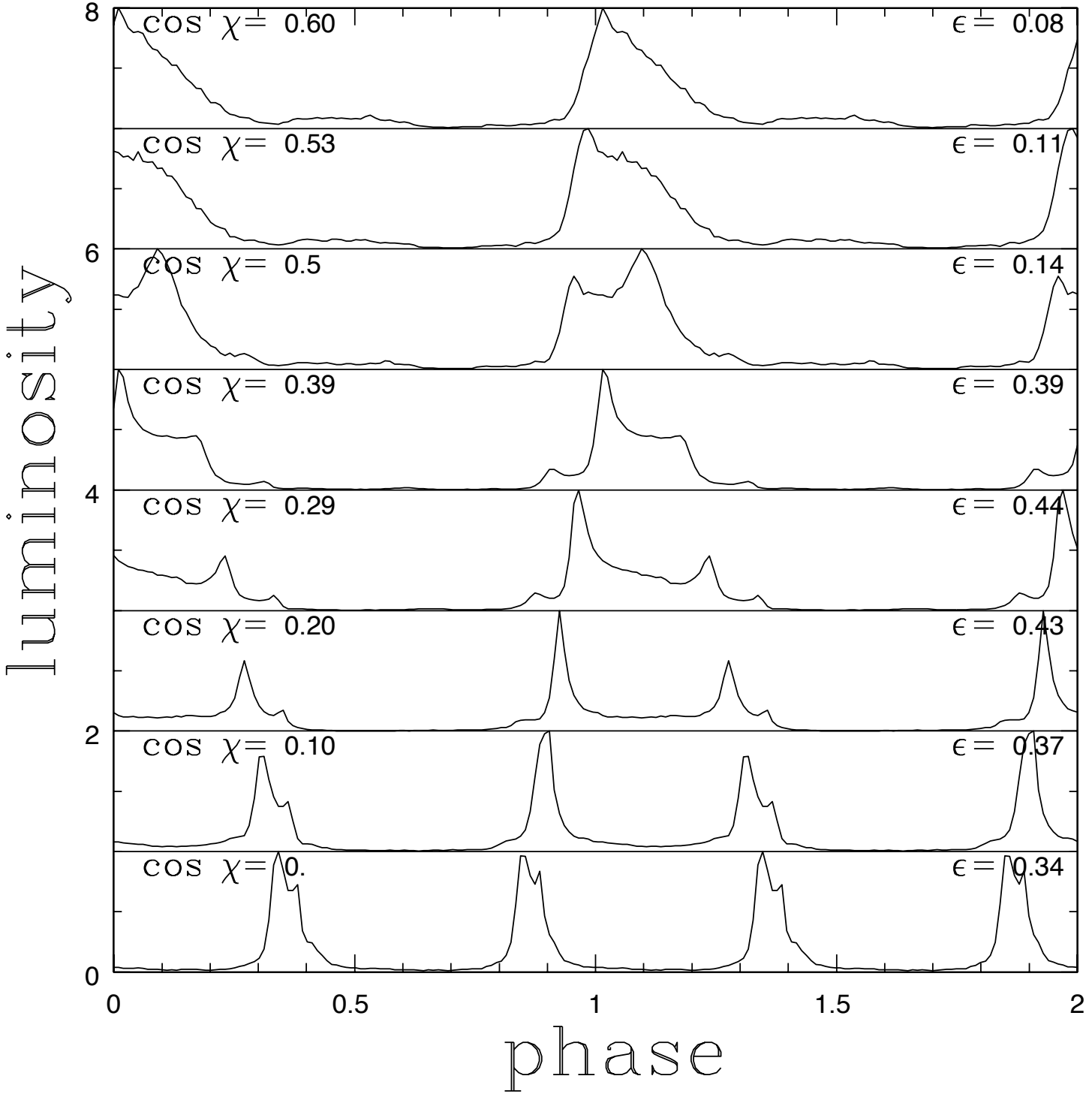
cos χ= 0.60
ϵ= 0.08
cos χ= 0.53
ϵ= 0.11
cos χ= 0.5
ϵ= 0.14
cos χ= 0.39
ϵ= 0.39
cos χ= 0.29
ϵ= 0.44
cos χ= 0.20
ϵ= 0.43
cos χ= 0.10
ϵ= 0.37
cos χ= 0.
ϵ= 0.34
luminosity
phase
0
2
4
6
8
0
0.5
1
1.5
2

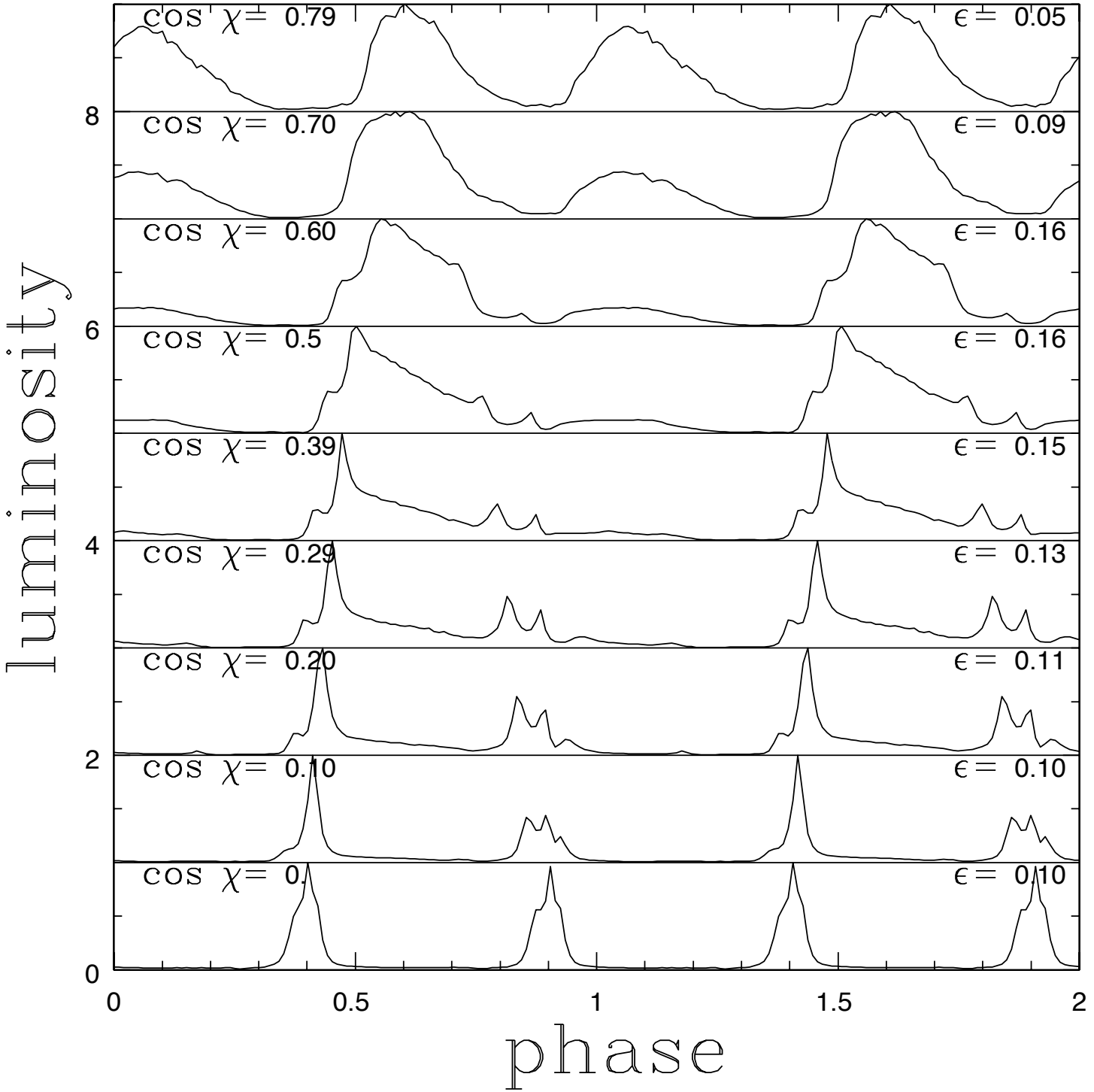
cos χ= 0.79
ϵ= 0.05
cos χ= 0.70
ϵ= 0.09
cos χ= 0.60
ϵ= 0.16
cos χ= 0.5
ϵ= 0.16
cos χ= 0.39
ϵ= 0.15
cos χ= 0.29
ϵ= 0.13
cos χ= 0.20
ϵ= 0.11
cos χ= 0.10
ϵ= 0.10
cos χ= 0.
ϵ= 0.10
luminosity
phase
0
2
4
6
8
0
0.5
1
1.5
2

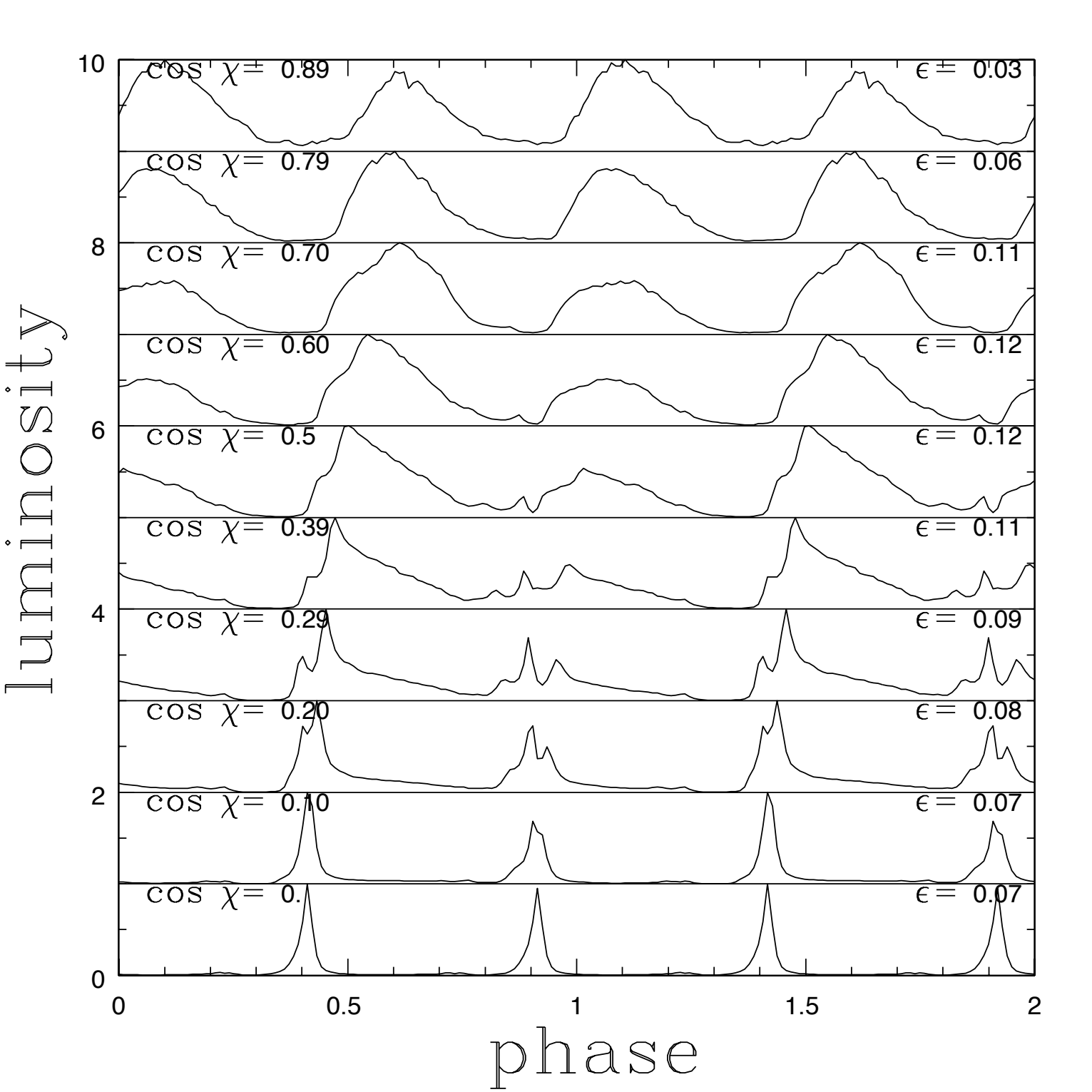
cos χ = 0.89
ϵ = 0.03
cos χ = 0.79
ϵ = 0.06
cos χ = 0.70
ϵ = 0.11
cos χ = 0.60
ϵ = 0.12
cos χ = 0.5
ϵ = 0.12
cos χ = 0.39
ϵ = 0.11
cos χ = 0.29
ϵ = 0.09
cos χ = 0.20
ϵ = 0.08
cos χ = 0.10
ϵ = 0.07
cos χ = 0.
ϵ = 0.07
luminosity
phase
0
2
4
6
8
10
0
0.5
1
1.5
2

Table 9. Spectral fitting results for young LAT-detected pulsars

PSR[a]	Photon Flux ($\mathrm{ph\,cm^{-2}\,s^{-1}}$) ($\times 10^{-8}$)	Energy Flux ($\mathrm{erg\,cm^{-2}\,s^{-1}}$) ($\times 10^{-11}$)	Γ	$E_{\rm cut}$ (GeV)	TS	$TS_{\rm cut}$	$TS_{\rm b\,free}$	Luminosity ($10^{33}\,\mathrm{erg\,s^{-1}}$)	Efficiency[b] (%)
J0007+7303	32.9 ± 0.4	40.1 ± 0.4	1.4 ± 0.1	4.7 ± 0.2	43388	1884	4	$94 \pm 1 \pm 40$	$21.0 \pm 0.2 \pm 8$
J0106+4855	1.7 ± 0.4	1.9 ± 0.2	1.2 ± 0.2	2.7 ± 0.6	544	58	2	$21 \pm 2^{+20}_{-8}$	$71 \pm 7^{+60}_{-30}$
J0205+6449	10.5 ± 0.7	5.4 ± 0.2	1.8 ± 0.1	1.6 ± 0.3	1019	86	7	$24 \pm 1 \pm 1.0$	$0.09 \pm 0.01 \pm 0.01$
J0248+6021	9.9 ± 1.3	5.2 ± 0.4	1.8 ± 0.1	1.6 ± 0.3	578	61	0	$25 \pm 2 \pm 5$	$12 \pm 1 \pm 2$
J0357+3205	9.0 ± 0.4	6.4 ± 0.2	1.0 ± 0.1	0.8 ± 0.1	3468	461	2	...	...
J0534+2200	208 ± 1	129.3 ± 0.8	1.9 ± 0.1	4.2 ± 0.2	102653	1461	13	$619 \pm 4 \pm 300$	$0.14 \pm 0.01 \pm 0.1$
J0622+3749	2.0 ± 0.3	1.4 ± 0.1	0.6 ± 0.4	0.6 ± 0.1	302	91	0	...	...
J0631+1036	6.4 ± 0.6	4.7 ± 0.3	1.8 ± 0.1	6 ± 1	621	39	1	$5.6 \pm 0.3^{+3}_{-2}$	$3.2 \pm 0.2^{+2}_{-1}$
J0633+0632	9.7 ± 1.1	9.4 ± 0.5	1.4 ± 0.1	2.7 ± 0.3	2448	203	9	...	...
J0633+1746	416 ± 1	423.3 ± 1.2	1.2 ± 0.1	2.2 ± 0.1	906994	33861	277	$31.7 \pm 0.1^{+90}_{-20}$	$97.4 \pm 0.3^{+300}_{-50}$
J0659+1414	7.1 ± 0.6	2.5 ± 0.2	1.7 ± 0.5	0.4 ± 0.2	419	33	0	$0.24 \pm 0.02 \pm 0.05$	$0.62 \pm 0.04 \pm 0.1$
J0729−1448 †	...	...	...	...	54	26	0	...	...
J0734−1559	10.8 ± 0.7	5.6 ± 0.2	2.0 ± 0.1	3.2 ± 0.9	916	39	9	...	...
J0742−2822	3.2 ± 0.6	1.7 ± 0.2	1.7 ± 0.3	1.6 ± 0.8	112	11	2	$9 \pm 1 \pm 4$	$6.2 \pm 0.7 \pm 3$
J0835−4510	1088 ± 2	906 ± 2	1.5 ± 0.1	3.0 ± 0.1	1659005	43084	916	$89.3 \pm 0.2 \pm 10$	$1.3 \pm 0.1 \pm 0.1$
J0908−4913	7.9 ± 1.3	4.4 ± 0.4	1.0 ± 0.4	0.5 ± 0.2	315	82	0	$35 \pm 3^{+30}_{-20}$	$7.1 \pm 0.7^{+6}_{-4}$
J0940−5428 †	...	...	...	...	14	13	8	...	...
J1016−5857	6.9 ± 2.4	5.4 ± 0.9	1.8 ± 0.2	6 ± 3	290	13	0	$55 \pm 9^{+30}_{-50}$	$2.1 \pm 0.4^{+1}_{-2}$
J1019−5749 †	...	...	...	...	21	0	0	...	...
J1023−5746	30 ± 3	19.5 ± 1.2	1.7 ± 0.1	2.5 ± 0.4	2926	162	20	...	...
J1028−5819	31 ± 2	24.3 ± 0.8	1.7 ± 0.1	4.6 ± 0.5	5096	235	28	$158 \pm 5 \pm 40$	$18.9 \pm 0.6 \pm 5$
J1044−5737	26 ± 1	15.6 ± 0.5	1.8 ± 0.1	2.8 ± 0.3	3380	202	19	...	...
J1048−5832	25 ± 2	19.6 ± 0.6	1.6 ± 0.1	3.0 ± 0.3	5389	325	30	$176 \pm 5 \pm 40$	$8.8 \pm 0.3 \pm 2$
J1057−5226	32 ± 1	29.5 ± 0.3	1.0 ± 0.1	1.4 ± 0.1	27848	2377	5	$4.3 \pm 0.1^{+5}_{-3}$	$14.4 \pm 0.2^{\pm}10$
J1105−6107	7.8 ± 1.6	4.9 ± 0.6	1.5 ± 0.3	1.3 ± 0.6	309	42	8	$150 \pm 20 \pm 50$	$5.9 \pm 0.7 \pm 2$
J1112−6103	1.9 ± 0.9	2.0 ± 0.5	1.6 ± 0.3	6 ± 3	58	6	0	$360 \pm 90^{+600}_{-200}$	$8 \pm 2^{+10}_{-4}$
J1119−6127	11 ± 2	7.1 ± 0.5	1.8 ± 0.1	3.2 ± 0.8	661	37	13	$600 \pm 40 \pm 60$	$26 \pm 2 \pm 2$
J1124−5916	10 ± 1	6.2 ± 0.4	1.8 ± 0.1	2.1 ± 0.4	1058	79	6	$170 \pm 10^{+50}_{-70}$	$1.4 \pm 0.1^{+0.4}_{-0.6}$
J1135−6055	7.4 ± 0.9	4.8 ± 0.3	1.7 ± 0.1	2.4 ± 0.5	498	61	3	...	...
J1357−6429	7.8 ± 1.1	3.4 ± 0.3	1.8 ± 0.4	0.9 ± 0.5	187	20	0	$25 \pm 2^{+10}_{-8}$	$0.82 \pm 0.08^{+0.4}_{-0.3}$
J1410−6132 †	3 ± 3	3 ± 1	...	...	40	9	0	$800 \pm 300^{+900}_{-400}$	$8 \pm 3^{+9}_{-4}$
J1413−6205	16 ± 2	15.7 ± 0.6	1.5 ± 0.1	4.1 ± 0.5	1795	180	1	...	...
J1418−6058	38 ± 3	30.2 ± 1.4	1.8 ± 0.1	5.5 ± 0.5	3487	172	1	$92 \pm 4^{+100}_{-60}$	$1.9 \pm 0.1^{+2}_{-1}$

How Pulsars Shine

calculating
understanding
} pulsars

Results :

→ can calculate weak* (to be defined) pulsars, standard candles

→ should be able to calculate non-weak pulsars

→ rough understanding of weak pulsars

No Results :

→ radio, other non-γ

→ ions

→ ~~[illegible]~~ understanding of strong pulsars